

# Experimental Study of Peripheral, Balloon-expandable Stent Systems

W. SCHMIDT, P. BEHRENS, D. BEHREND, K.-P. SCHMITZ  
Institute for Biomedical Engineering, University of Rostock, Rostock, Germany

R. ANDRESEN  
Department of Radiology, Güstrow Municipal Hospital, Academic Teaching Hospital, University of Rostock, Güstrow, Germany

## Summary

*Five balloon-expandable stents and their accompanying balloon catheters were studied regarding their geometric and mechanical characteristics (Biotronik Peiron, Cordis Corinthian IQ, Guidant OTW Megalink, Inflow Dynamics Antares, Medtronic AVE Bridge). The measurements obtained for profile, elastic recoil, stent foreshortening, trackability, flexural strength crimped and expanded, as well as X-ray contrast are compared and discussed from the point of view of possible clinical use.*

## Key Words

Peripheral balloon-expandable stents, biomechanical study, interventional radiology

## Introduction

Lately, vessel stenoses are being treated increasingly with scaffolding prostheses if the primary result following angioplasty indicates residual stenosis or vessel dissection [1-4]. Stent sizes and designs adapted to the special application sites are being used. For the most part, vascular stents are used for the coronary vessels, the renal arteries, pelvic vessels, leg arteries, and the carotid artery. Besides the principle of self-expanding stents, balloon-expandable stent systems are becoming widespread in many areas. They can be positioned with precision and, when expanded, can facilitate the application of high pressure on the vessel wall. From the standpoint of structural mechanics, there are no essential differences between coronary and peripheral stents. As a rule, the different application sites and the larger vessel diameters within the periphery require appropriate stent diameters.

In this study, five currently marketed, balloon-expandable stents, including their delivery systems (SDS), were subjected to a comparative test. Their mechanical and geometric qualities were measured and assessed by utilizing the same criteria that are currently used to evaluate coronary stent systems [5-10].

## Materials and Methods

Balloon-expandable stents of a comparable dimension were selected. All systems show a nominal diameter of 8 mm and a stent length of between 38 and 40 mm. A special case is the Cordis Corinthian stent: its nominal stent length already takes into account its foreshortening during expansion to 8 mm; therefore, the system is listed as 8.0 x 29 mm. All stents are of the so-called "slotted-tube" type with considerable differences in the design of the functional elements and their association with each another (Figure 1). Megalink (Guidant, USA), Bridge (Medtronic, USA), and Peiron (Biotronik, Germany) have segment series that are connected with one another by individual bridges. In comparison, the Antares (InFlow Dynamics, Germany) and the Corinthian (Johnson & Johnson, Canada) stents have completely connected elements.

The metrological recording of the characteristic qualities of stent and balloon catheters was carried out with various special devices that have already been used in the testing of coronary stent systems, and, within this context, were also published [5,6]. Therefore, the essential measurement principles will be named only briefly. The measurement of the system's trackability was per-

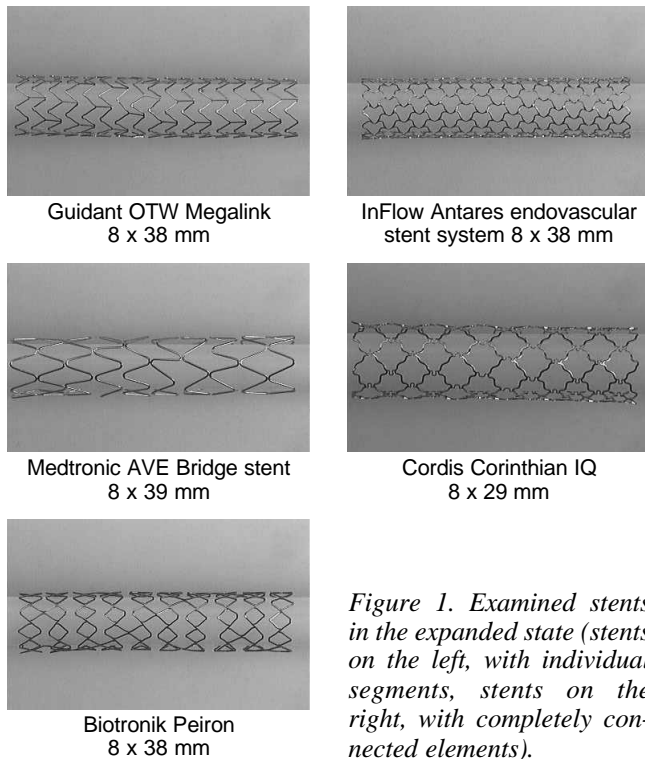


Figure 1. Examined stents in the expanded state (stents on the left, with individual segments, stents on the right, with completely connected elements).

formed using a motor-driven advancement of the complete SDS through a testing route adapted to the anatomical relationships of different vascular provinces (Figure 2). The comparison with angiographic projections of the renal artery branching, intersections of the large vessels from the aortic arch, and the pelvic arteries shows a good agreement of the essential distances and curve radii (Figure 3). The area between points C and E of the model would correspond to the anatomical relationships of the aorta's bifurcation and can serve as a so-called crossover model between the right and left A. iliaca com.

The advancement was accomplished using a Boston Scientific Starter 0.035" guide wire (exception: 0.014" with the Guidant Megalink, which is designed for 0.018" maximum guide wires) and measured using the required proximal thrust. This results in trackable force curves which allow to assign the prominent points of the testing range to measured force values, and thereby to assess typical tracking qualities.

The measurements of stent expansion and recoil, as well as the system profile in the crimped stage, were performed without touching the stent and with the use of a special laser measurement system [5]. The stent was expanded in separate pressure steps ranging from

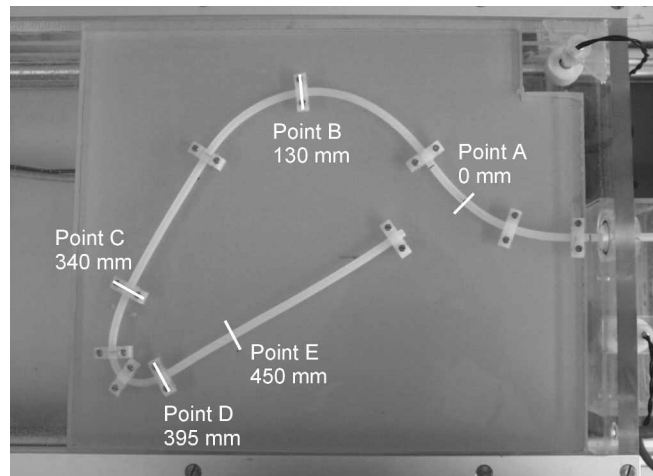


Figure 2. Testing route for the comparative measurement of trackability for peripheral stent systems.

2 bar up to the rated value of the stent system. By scanning the stent range in 0.5 mm steps at the given pressure steps, expansion profiles could be obtained that were able to supply information as to the current stent diameter, and thus served as a basis for calculation of the elastic recoil. The average stent diameter during the individual pressure steps of expansion and after the subsequent release of pressure were calculated by taking the arithmetic average  $\bar{d}$  of the diameters  $d_{RMS}(z)$  resulting from the profile measurements. The following definitions are used:

$$d_{RMS}(z) = \sqrt{\frac{d_x^2(z) + d_y^2(z)}{2}}$$

$$\bar{d} = \frac{1}{n} \sum_{z=z_a}^{z_e} d_{RMS}(z)$$

Here  $d_x$  and  $d_y$  are the individual measured values for the x- and y-projections,  $z_a$  and  $z_e$  are the first and last measured points on the stent, and  $n$  is the number of measured points at the stent.

To test the radial strength of the stent, the stent is used in the test setup that is described more extensively in [5]. The stent, implanted in a thin-walled tube (Pellethane, I.D. = 8.0 mm, wall thickness = 0.075 mm) is placed in a tempered test basin. The pressure in the test basin is increased to 1.5 bar in steps of 0.1 bar. This pressure creates a radial load on the tube around the stent until the stent collapses.

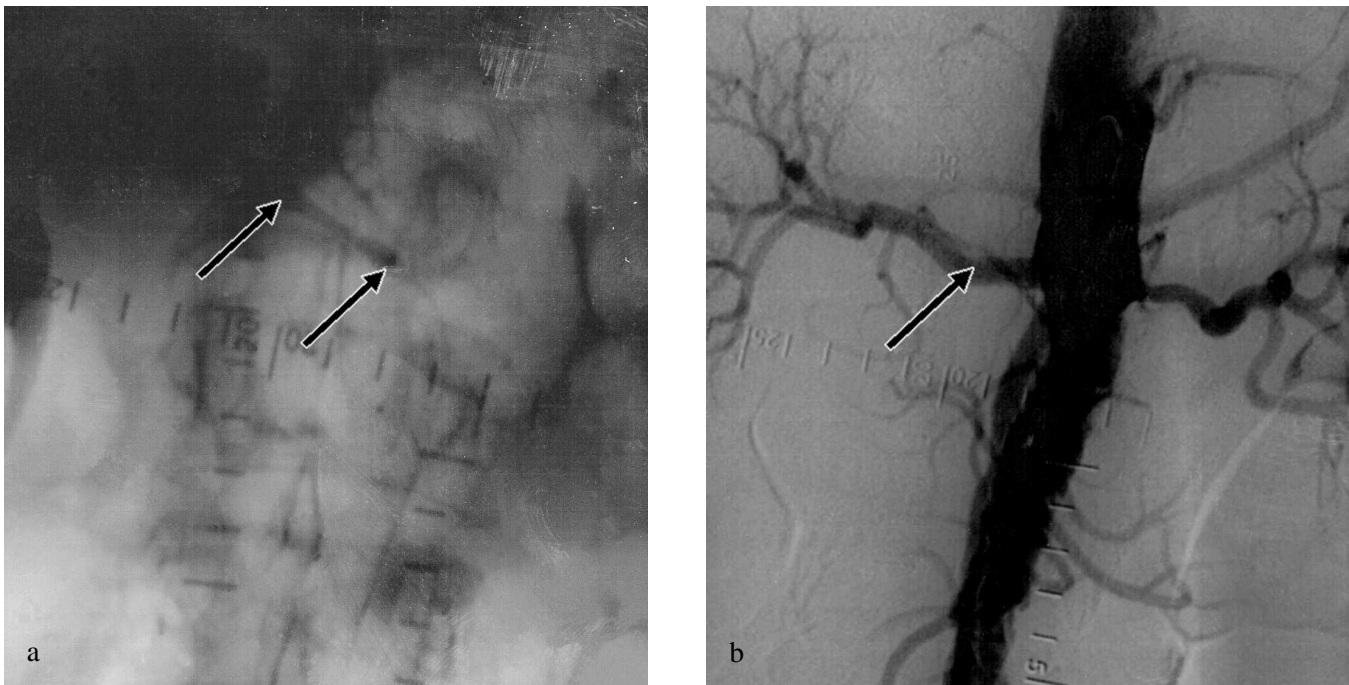


Figure 3. Renal artery PTA with stent application: a) the positioned, but not yet fully expanded stent in the renal artery stenosis; the stenosis access correlates with the curvature in area B of the vascular-model; b) post-interventional image with completely removed stenosis and completely deployed stent prosthesis.

The measurement principle for determining the flexural strength of the expanded stent is depicted in Figure 4. The flexural strength  $EI$  of the stent is determined by reconstructing the relationship between the bending deflection ( $f$ ) and the point force ( $F$ ), based on the general bending theory for a cantilever:

$$EI = \frac{F \cdot l^3}{3f}$$

In order to consider the influence of stent geometry, the measurements of the flexural strength for all stents are performed at 5 measurement points, each shifted by  $45^\circ$  along the perimeter. Three measurements are performed at each measurement point in order to reduce random measurement error. The resulting flexural strength for each stent is given averaged over the entire range.

The stent length before and after expansion is tested with a digital caliper gauge (Mitutoyo). The change in length is calculated as the difference between the two values.

The X-ray density of the expanded stent was determined with the analogous device Siemens Mobilett,

with a 7:1 scatter-ray grid at a high-voltage of 70 kV and a basic setup as per DIN V 13273-7:1996-12, Section 6 (Figure 5). The distance between the radiation source and the film (film focal distance) was 1150 mm. The distance between the focus and the test object depends on this distance and the scattering body thick-

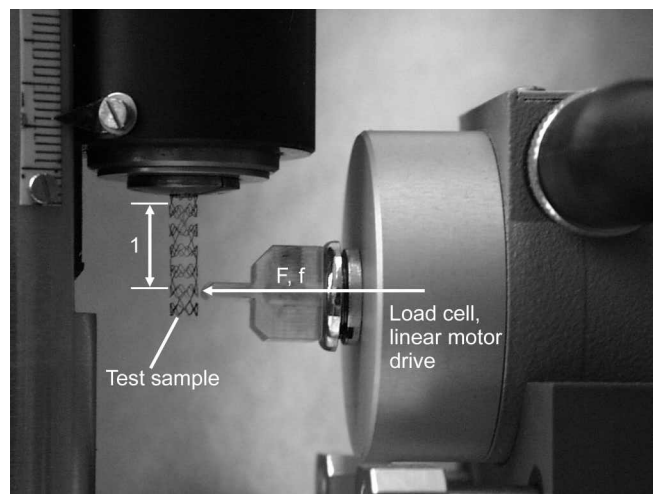


Figure 4. Test setup for measurement of flexural strength.

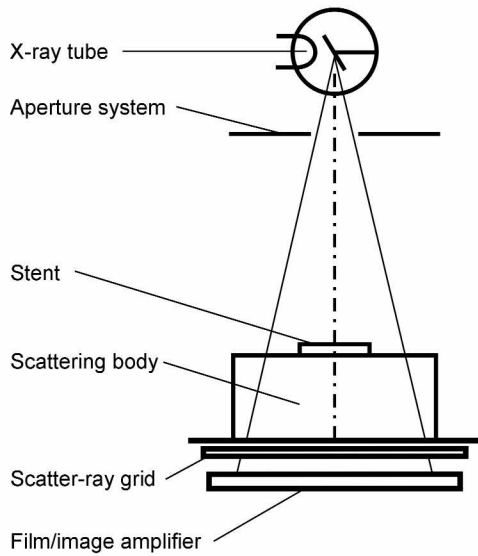


Figure 5. Measurement setup for determining the attenuation of X-ray radiation as per DIN V 13273-7.

ness of 150 mm (PMMA) and was 1000 mm accordingly. The quantitative evaluation was performed by scanning the film (HP ScanJet 6100) with fixed settings for brightness, contrast, and resolution. The gray

tones were determined for the stent body ( $G_s$ ), SDS markers ( $G_{bm}$ ), and the immediately adjacent film area ( $G_f$ ) without an object. The characteristic values  $K$

$$K_s = \frac{G_s}{G_f} - 1$$

$$K_{bm} = \frac{G_{bm}}{G_f} - 1$$

are appropriate for comparison as a measure for the X-ray contrast.

### Results

The trackability measurement of the five examined stent systems provided trackable force curves, as shown in Figure 6. A quantitative evaluation was carried out by calculating the strength mean values over the measuring path. The results for the total measuring path of  $s = 450$  mm (measurement points A to E) are presented graphically in Figure 7. If the passage of the strongest curve (advancement corresponding to the crossover technology in the area of the pelvic arteries)

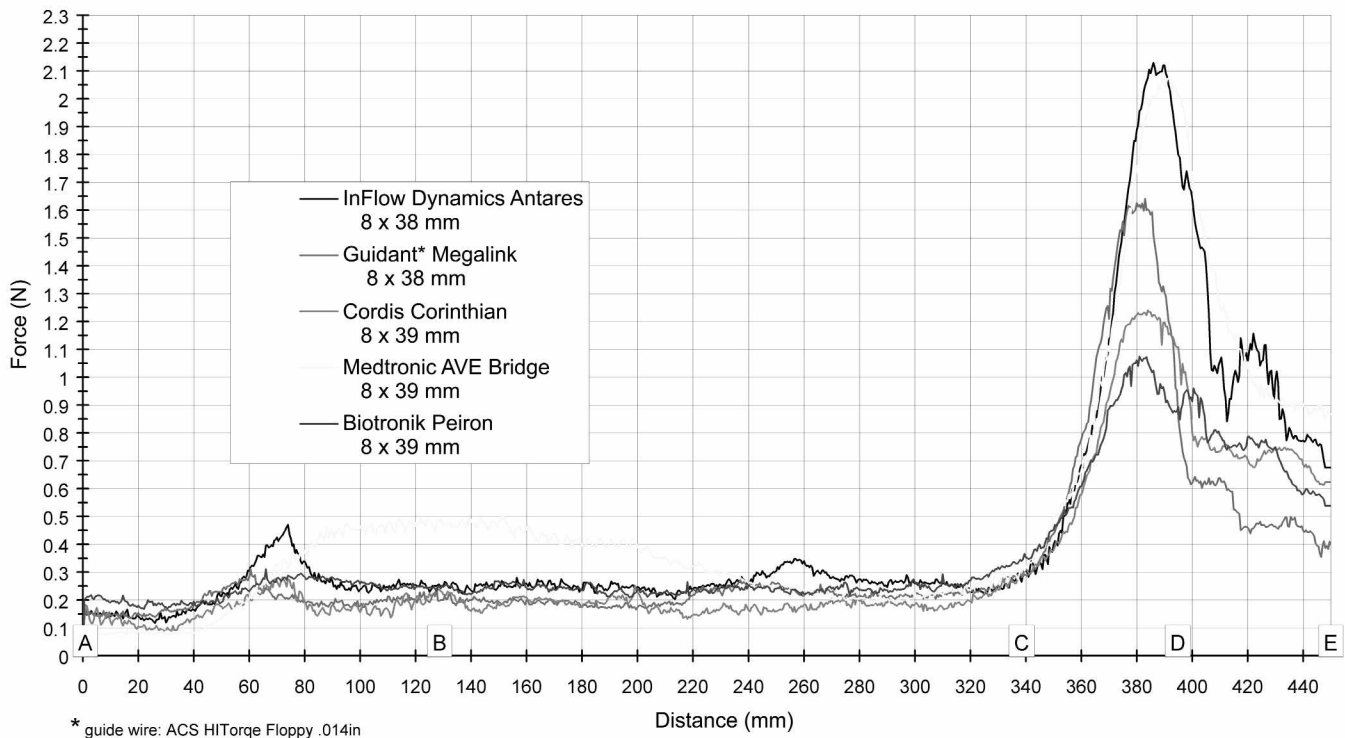


Figure 6. Trackable force curves of the track test for all systems.

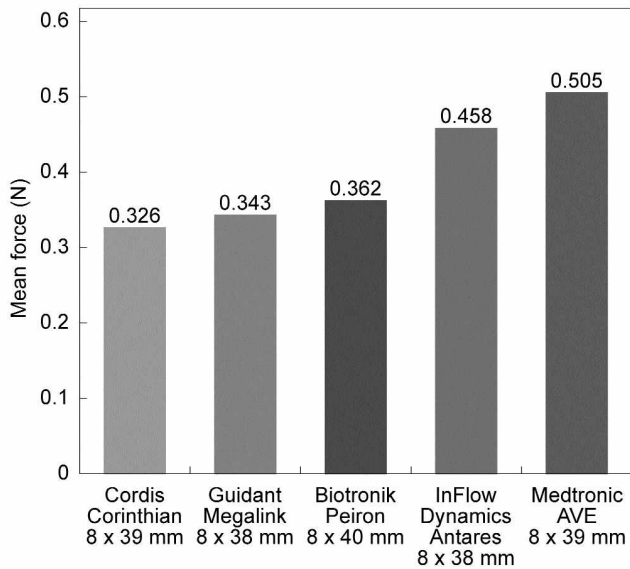


Figure 7. Mean trackable force over the total test route (450 mm from A to E).

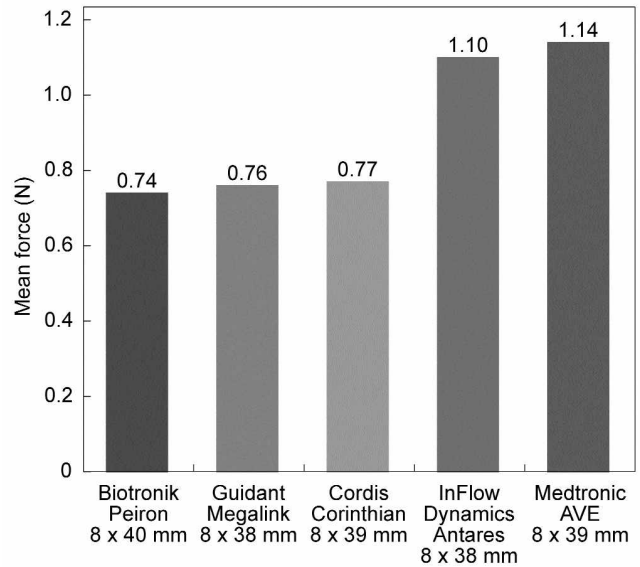


Figure 8. Mean trackable force over the test route from C to E (110 mm).

is selected as a criterion, the strength mean values from point C to E are obtained in accordance with Figure 8. Besides good trackability qualities, the passage of possibly calcified vascular constrictions also requires a good profile of the SDS, especially of the catheter tip, the distal balloon shoulder, and the distal transition from the

balloon to the stent area. A geometric assessment of this distal profile of the complete system is possible with the help of Figure 9, which presents the relevant sections of the five examined systems in graphic form. While the Bridge system has by far the largest profile in the stent region (2.430 mm) but no distinguishable balloon should-

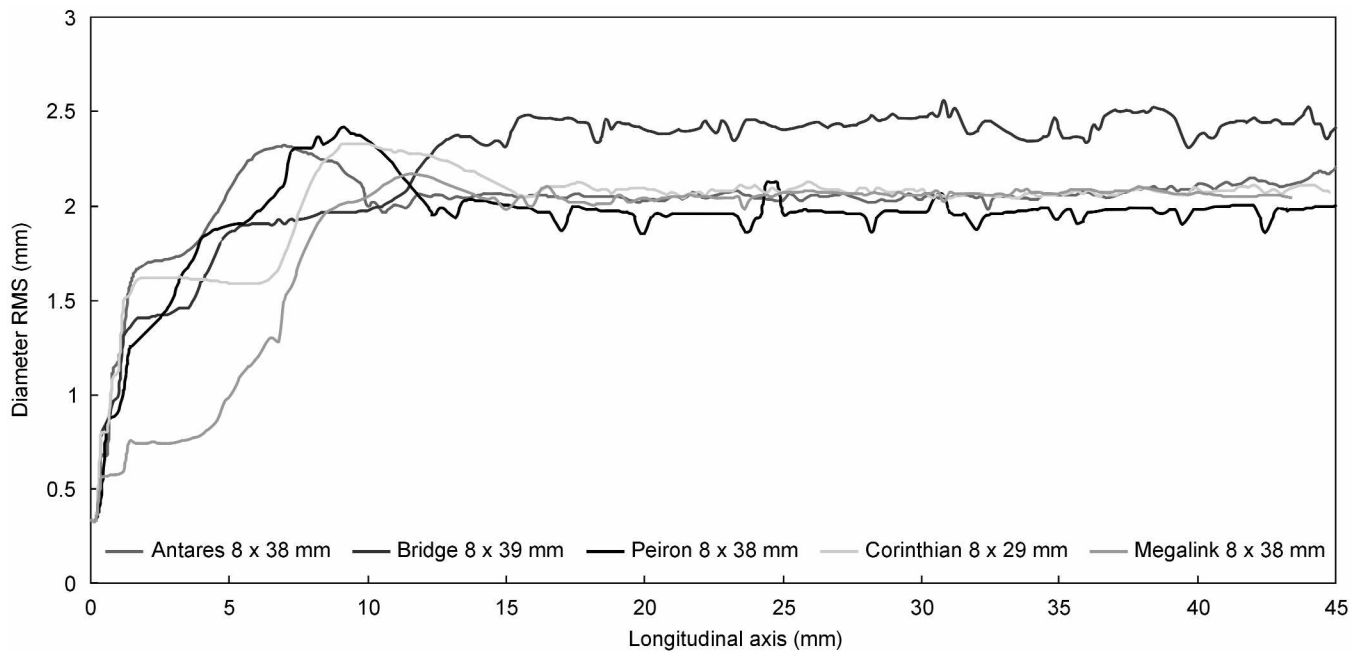


Figure 9. Distal profile of the stent systems with a crimped stent.

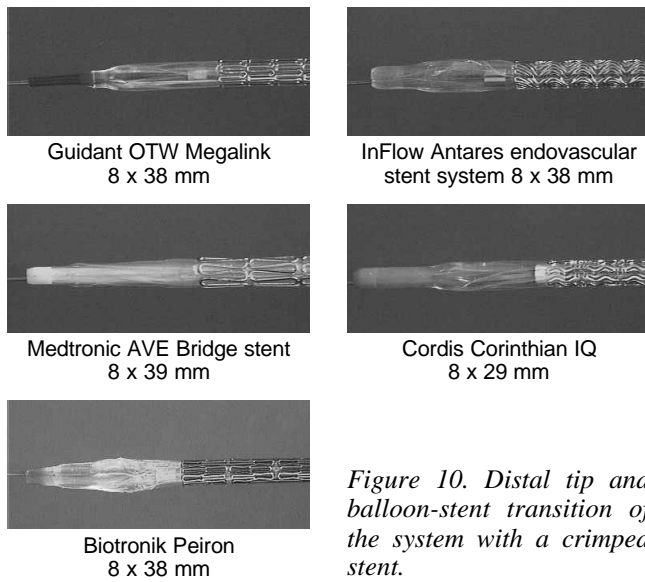


Figure 10. Distal tip and balloon-stent transition of the system with a crimped stent.

der, all other systems have a clearly smaller profile in the stent region. The smallest values were measured for the Peiron stent (1.970). With Megalink, Antares, and Corinthian, the mean diameters in this area are only slightly above it (2.056 to 2.078 mm). The balloon shoulder is clearly recognizable in three systems in the profile (Antares, Corinthian, Peiron: 2.318 to 2.415 mm maximum diameter), with Megalink only as a bulge of at most 2.168 mm. Figure 10 provides additional detailed photos of the distal SDS.

A comparison of the measured flexural strength in the distal area of the SDS with a crimped stent shows the Megalink having the least flexural strength (394.5 Nmm<sup>2</sup>), while the Bridge system is the stiffest (471.6 Nmm<sup>2</sup>). The remaining three systems, which have a flexural strength of EI = 427-430.6 Nmm<sup>2</sup>, show an approximately equal stiffness response (Figure 11). The elastic recoil after expansion is always an important characteristic value for balloon-expandable stents. The measured values are presented graphically in Figure 12. The recoil values for the Corinthian, Antares, Megalink, and Peiron are between 2.5 and 3.5 %. In comparison, the Bridge stent shows recoiling that is more than 35 % higher (4.79 %).

Figure 13 shows a graphic display of the pressure at the point of failure  $p_{coll}$  for the stent types studied. Here the Corinthian stent is clearly stronger in regard to radial load through a surrounding vessel than the other examined types. Figure 14 gives an overview of the average flexural strength of the expanded stents for each stent type (averages around the perimeter). The Corinthian and Antares stents (462.9 and 485.7 Nmm<sup>2</sup>, respectively) show the greatest stiffness, the Bridge and Megalink are in the middle region with 269.2 and 280.9 Nmm<sup>2</sup>, respectively, while the Peiron is the most flexible with 141.18 Nmm<sup>2</sup>. Figure 15 provides information as to the percent change in the stent length upon stent expansion when drawn as compared to the length

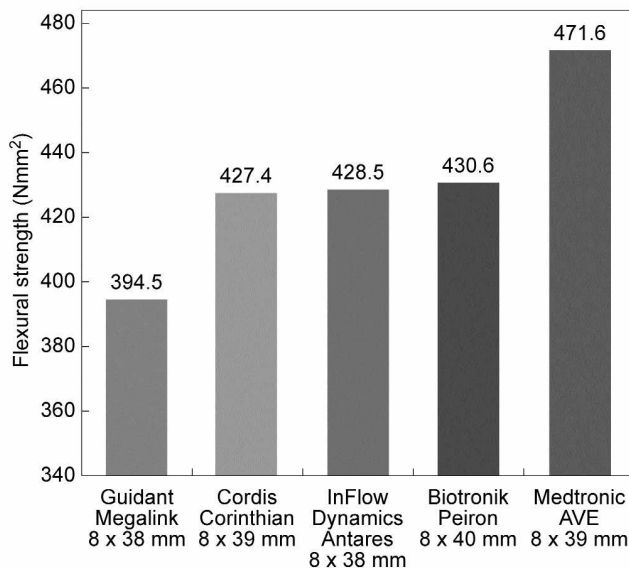


Figure 11. Flexural strength of the complete SDS in the area of the crimped stent.

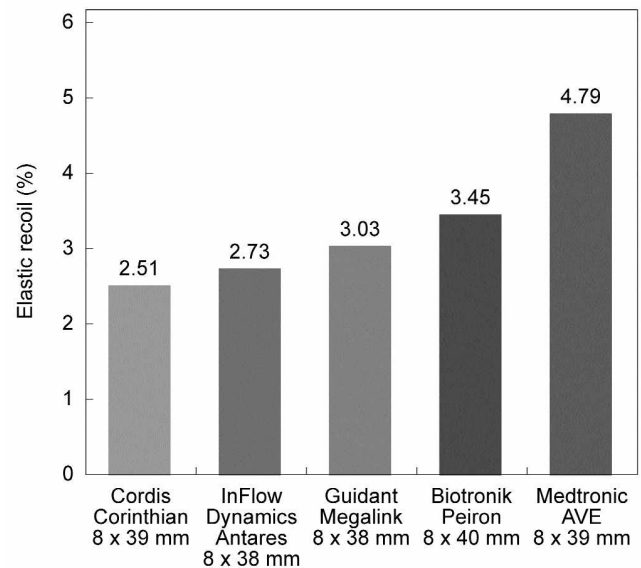


Figure 12. Recoil of stent systems studied after expansion at nominal pressure.

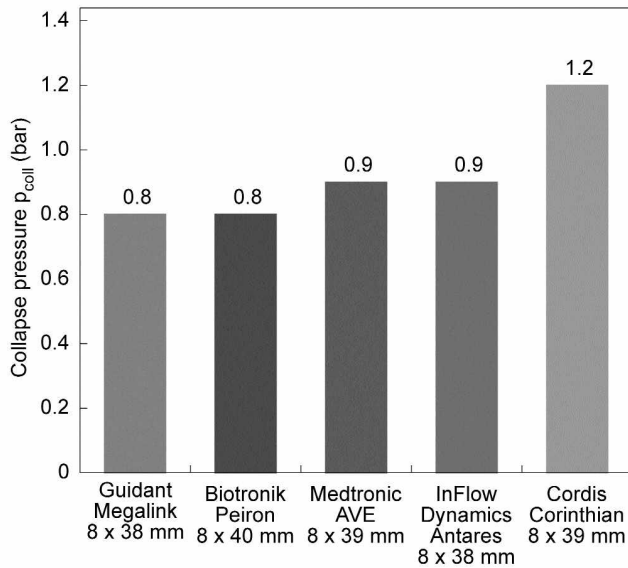


Figure 13. Pressure required to induce collapse for the examined stent types.

of the stent type when contracted. Above all, what is most apparent here is the considerable reduction of the Corinthian stent with complete expansion. The X-rays of the stent systems studied are displayed in Figure 16. The expanded stents imaged under the same conditions are seen in Figure 17. Figure 18 shows

a comparison of the calculated contrast values  $K$  for the crimped stents on SDS. A high value for  $K$  means good visibility;  $K = 0$  means that the lightness of the object and film is exactly the same, i.e. the object is not visible. The same image analysis was done for the expanded stents and yielded the results shown in Figure 19.

**Discussion**

The current status in the technology of peripheral stents offers self-expandable and balloon-expandable types for many applications. Both principles do not concur directly with each other, but rather complement one another in their features and area of application. As a rule, balloon-expandable stents can be positioned with safety and precision, while the expansion of the stenosis can be effected by a great force due to the expanding balloon; and they exhibit good X-ray density [1,3]. The aim of the present study was to measure the essential geometric and mechanical characteristics of commercially available, balloon-expandable stents and to compare them. A comparison to the literature [7,8] is difficult for many characteristic qualities since, the measurement conditions are not standardized. It can be stated that, in general, systems with less trackable force have advantages with regard to reach-

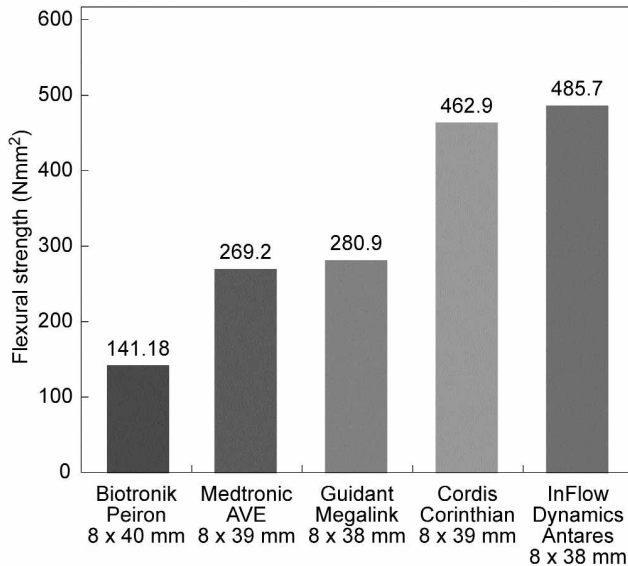


Figure 14. Average flexural strength of stents expanded to 8 mm nominal diameter.

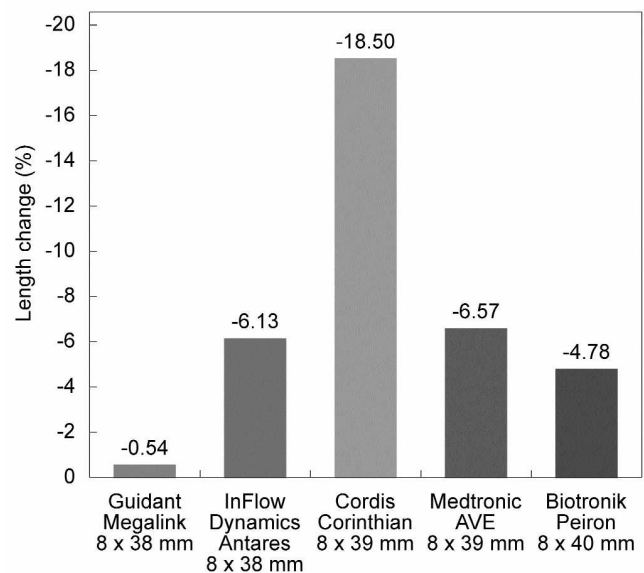


Figure 15. Percent change in length of stent systems studied after expansion to the nominal value (for each stent type).

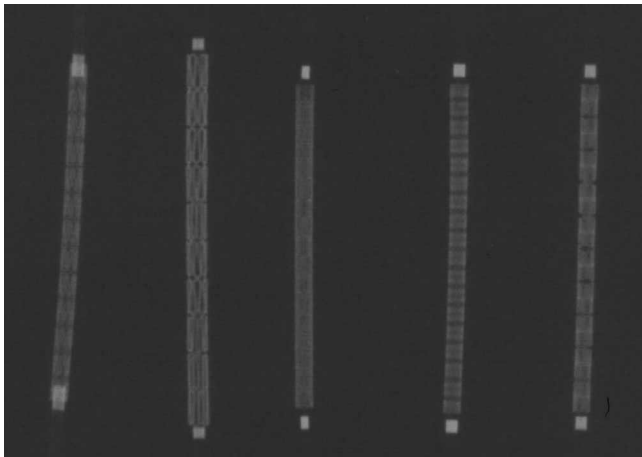


Figure 16. X-ray of peripheral stent systems with crimped stents - From left to right: Corinthian IQ (Johnson & Johnson, Canada), Bridge (Medtronic, USA), Megalink (Guidant, USA), Antares (InFlow Dynamics, Germany), Peiron (Biotronik, Germany).

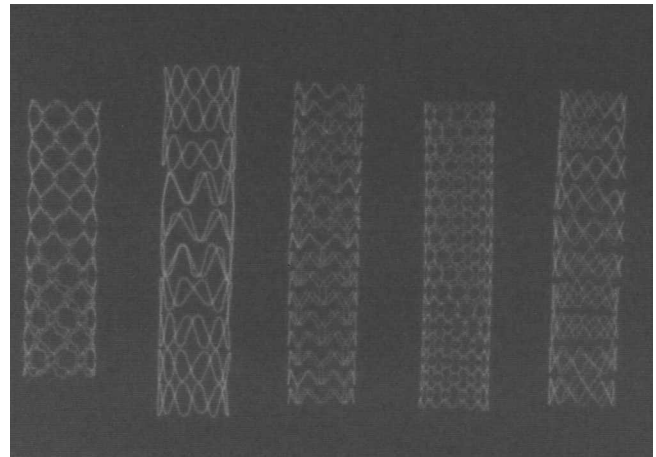


Figure 17. X-ray of expanded peripheral stents - From left to right: Corinthian IQ (Johnson & Johnson, Canada), Bridge (Medtronic, USA), Megalink (Guidant, USA), Antares (InFlow Dynamics, Germany), Peiron (Biotronik, Germany).

ing the target lesion, especially if access to the lesion is not directly possible. Consequently, the derived mean values for trackable force are dominated justifiably by the high measured values of the most severe curvature (model for renal artery branching, branching of the large vessels from the aortic arch and the aorta's bifurcation with crossover technology), so that the Corinthian, Megalink, and Peiron systems appear to

be consistently better in trackability than the Bridge or Antares systems. It is also noteworthy that the Megalink system could only be tested on a 0.014" guide wire since the guide wire lumen is designed for a 0.018" maximum. A thinner wire can have a negative influence on trackability since it is less stiff than a guide wire that is more than double in size and, therefore, offers less guidance. On the other hand,

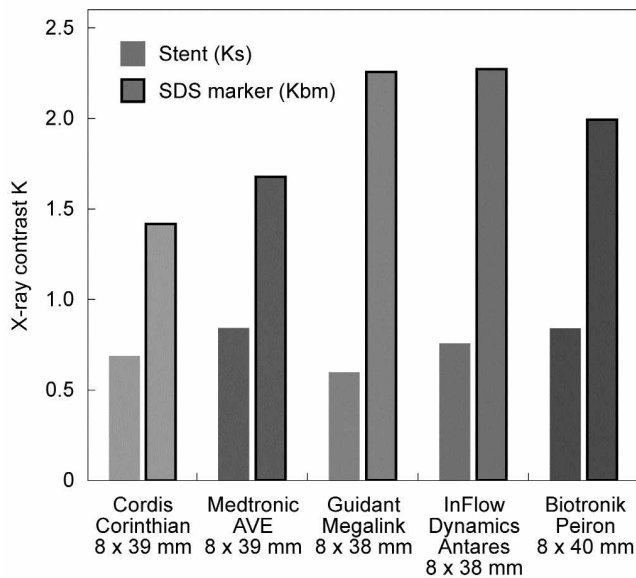


Figure 18. X-ray contrast of peripheral stent systems with crimped stents.

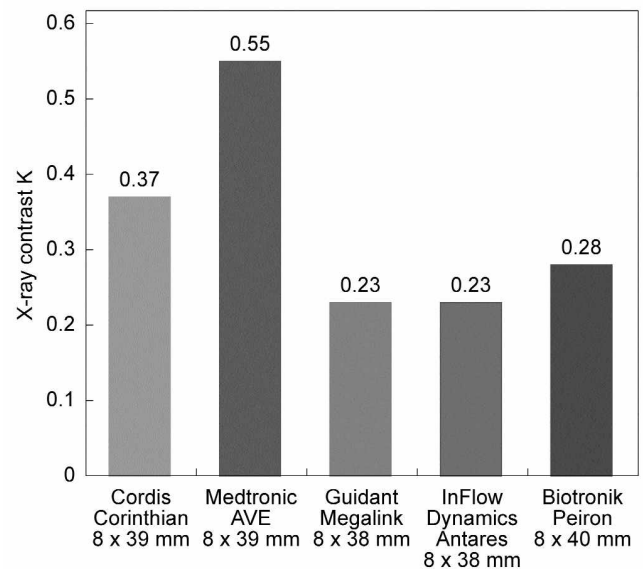


Figure 19. X-ray contrast of peripheral stents in the expanded state.



with passages around strong curvatures, the higher flexibility is definitely advantageous because the normal stresses between SDS and vascular wall are reduced.

In the measured profile of the stent systems, the Bridge stent was most noteworthy since in the crimped state it showed a clearly larger profile than all other examined stent systems, which indicated a similar diameter only in the area of the distal balloon shoulder. At the same time, balloon shoulders that limit the stent on both sides are sometimes also regarded as additional security against an unwanted dislocation of the stent during advancement. When introducing the stent system into a narrow stenosis, this shoulder can also be a nuisance, and if it is less flexible, it can have a negative influence on the crossing features. However, the small calipers of the stent delivery systems (SDS) that are desirable in the coronary region and are sometimes limiting play a subordinate role with the large diameters of the vessels in the periphery, as long as the actual vascular access (lead introducer, guiding catheter) can be kept small.

The shape of the distal catheter tip may likewise be significant for assessing the trackability and crossing profile features. Here the measured systems indicate differences, for example, in the shape of the balloon tip (distal tubing), but also in the profile across the balloon's transition to the tubing.

The correlation of flexural strength of the distal tip of the stent system with the measured track strengths is not easy to accomplish. That becomes clear with the Antares, which indicates the same flexural strength as the Corinthian or the Peiron, and nevertheless provided comparatively high strengths in the track test. In comparison with the Bridge system, a correlation with the characteristic value of the flexural strength in the crimped state can also be presumed for the Megalink, Corinthian, and Peiron systems. Flexible stents can pass narrow radii better.

The stent recoil is an important characteristic of all balloon-expandable stents. Types with small recoil values guarantee a large acute lumen with minimal strain on the vessel, and thus reduce the risk of incisions or even ruptures of the vessel wall. This parameter can also be important with regard to flow disturbances and pressure gradients which may cause thrombus formation and postinterventional restenosis [12]. All examined stents showed an elastic recoil of  $< 5\%$ , and within these limits the Bridge stent showed the highest value (4.79 %).

It is expected of flexible stents that they adjust optimally to the vessel wall both at bends and during movement, and thus cause less vessel irritation. On the other hand, there are a couple of applications of peripheral stents where only less motion is expected and stiff stents will be suitable. For applications with highly mobile vessels or curved stenoses, self-expandable stents as a rule are preferable to balloon-expandable models.

High radial strength could be determined with all measured stents. The stents withstood an outer pressure of 0.7 to 1.1 bar, which represents for many vessels a large margin of safety. In areas where unsymmetrical and unphysiologically high loads on the stent by external influences must be expected, balloon-expandable stents should be avoided anyway.

The only slight change in length with the expansion of balloon-expandable stents described in [1] and [3] generally cannot be confirmed for the examined stents. The Corinthian, which shortens its length by more than 18 % with an expansion of 8 mm, is especially noticeable here. This change in length is documented by the manufacturer and, therefore, can be taken into account when implanting. In the immediate proximity of the intersections of large vessels, a less variable system is nevertheless to be used more conveniently.

Fluoroscopic contrast differs between the brands investigated, but at least the markers of the balloon are well visible so the placement of the stents will not be limited by X-ray contrast. The contrast of the expanded stents is lower than on the SDS but may still be sufficient. The visibility is not determined only through contrast, but also by the size of the visible surface [11]. Furthermore, with the projection of the border areas, material overlapping appears, which enhances the contrast along the outer contour of the stents [8]. This is advantageous for assessing the unfolding of the stent.

In summary, it can be stated that the parameters that were studied are well suited for a biomechanical assessment. However, care must be taken that the assessment is carried out for various applications with proper specific weighting.

## References

- [1] Jahnke T, Brossmann J, Voshage G, et al. Mid-term follow-up after placement of the new balloon-expandable VIP-stent into the iliac arteries. *RöFo - Fortschritte auf dem Gebiet der Röntgenstrahlen und der bildgebenden Verfahren*. 2000; 172: 381-385.

- [2] Link J, Muller-Hulsbeck S, Hackethal S, et al. Midterm follow-up after Cragg stent placement in iliac arteries. *RöFo - Fortschritte auf dem Gebiet der Röntgenstrahlen und der bildgebenden Verfahren*. 1997; 167: 412-417.
- [3] Muller-Hulsbeck S, Grimm J, Jahnke T, et al. First results after implantation of the new balloon-expanded Bridge-Stent into the iliac artery. *RöFo - Fortschritte auf dem Gebiet der Röntgenstrahlen und der bildgebenden Verfahren*. 2000; 172: 836-841.
- [4] Schurmann K, Haage P, Chalabi C, et al. The Perflex stent, a new balloon-expandable vascular stent: The initial clinical results. *RöFo - Fortschritte auf dem Gebiet der Röntgenstrahlen und der bildgebenden Verfahren*. 1999; 170: 497-502.
- [5] Schmidt W, Behrens P, Behrend D, et al. Measurement of mechanical properties of coronary stents according to the European Standard prEN 12006-3. *Prog Biomed Res*. 1999; 4: 45-51.
- [6] Schmitz K-P, Behrend D, Behrens P, et al. Comparative studies of different stent designs. *Prog Biomed Res*. 1999; 4: 52-58.
- [7] Dyet JF, Watts WG, Ettles DF, et al. Mechanical properties of metallic stents: How do these properties influence the choice of stent for specific lesions? *Cardiovasc Intervent Radiol*. 2000; 23: 47-54.
- [8] Schmiedl R, Schaldach M. X-ray imaging of coronary stents. *Prog Biomed Res*. 2000; 5: 184-196.
- [9] Schmitz K-P, Schmidt W, Behrens P, et al. In-vitro examination of clinically relevant stent parameters. *Prog Biomed Res*. 2000; 5: 197-203.
- [10] Dumoulin C, Cochelin B. Mechanical behaviour modelling of balloon-expandable stents. *J Biomech*. 2000; 33: 1461-1470.
- [11] Haas R. Implantation and imaging of coronary stents. *Radiol Technol*. 1996; 67: 233-244.
- [12] Müller-Hülsbeck S, Grimm J, Jahnke T, et al. flow pattern from metallic vascular endoprosthesis: in vitro results. *Eur Radiol*. 2001; 11: 893-901.

**Contact**

Dr. W. Schmidt

Universität Rostock

Institut für Biomedizinische Technik

Ernst-Heydemann-Strasse 6

D-18055 Rostock

Germany

Telephone: +49 381 54 34 55 08

Fax: +49 381 49 47 602

E-mail: wolfram.schmidt@medizin.uni-rostock.de